Electronic Supplementary Material (ESI) for Molecular Systems Design & Engineering.
This journal is © The Royal Society of Chemistry 2019

A General Formulation Approach for the Fabrication of Water Repellent Materials: How Composition can Impact Resilience and Functionality

R. L. Upton, Z. Davies-Manifold, M. Marcello, K. Arnold, C. R. Crick*

Electronic supplementary material (ESI†)

Materials: Sylgard-184 (Silicone elastomer) was purchased from Ellsworth Adhesive Ltd. High molecular weight polyvinylchloride (product number 81387), high density polyethylene (product number 547999), polypropylene (Mw~340000), silicon dioxide nanopowder (10-20 nm), fumed silica (0.2-0.3 μm average particle size), silica gel spherical (40-75 μm), titanium dioxide (Aeroxide P25, 21nm), cerium oxide (<25nm), oleic acid, triethylamine (>99%) and hexamethyldisilazane (reagent grade, ≥99%) were purchased from Sigma Aldrich. Lucigenin (10,10'-Dimethyl-9,9'-biacridinium dinitrate) and Nile Red (9-(Diethylamino)-5*H*-benzo[*a*]phenoxazin-5-one) were purchased from Tokyo Chemical Industry UK Ltd. Hexane (HPLC grade), tetrahydrofuran (99+%, extra pure, stabilized with BHT), xylene (analytical reagent grade), toluene (99.8+%) and ethanol (analytical reagent grade) were purchased from Fisher Scientific Limited. Plasticized-PVC coated fabric was purchased from Amazon (Fabrics 2 Cover).

Analysis: Surface morphologies of coatings were analysed using a scanning electron microscope (JEOL JSM-7001F) operating at an acceleration voltage of 10-20 kV. Samples were vacuum sputter coated in a thin layer of chromium to improve electrical conductivity. FTIR measurements were taken using a Bruker Optics' Vertex 70 over a range of 500 to 4000 cm^{-1}. Static WCA measurements were taken using a DSA100 Expert Drop Shape Analyser using sessile drop and Young-Laplace operating modes (manual setting to record WCA's); 6 μL water droplets were used and 5 measurements were taken for each sample. Confocal fluorescence microscopy was carried out using a Zeiss LSM710 on a Zeiss Observer Z1 (Zeiss, Jena, Germany) with a 40x /1.2 NA W Korr and a 63x/1.40 oil objectives. Samples were excited using an argon ion laser at 488 nm and a DPSS 561 nm laser. Data was captured using ZEN software (Zeiss, Jena, Germany). 3D volumetric data consisting of 57 z slices (SiO_2-PDMS) was processed with Imaris x64 8.4.2(Bitplane A.G., Zurich, Switzerland). Segmentation of the data was performed with grain size of 0.200 μm, and manual threshold and morphological parameters were measured. Images were stored and managed using OMERO software. Cross-sections were prepared in a focused ion beam (Tescan S8000G), using a gallium ion source.

The ion beam was operated at between 30 kV and 5 kV, and at beam currents ranging between 20 nA and 250 pA. A strap of platinum was deposited on to the surfaces of interest prior to milling, in order to minimise damage.

S1 Experimental methods

2.1 Hydrophobization of silica

A solution of HMDS (1 mL) in toluene (100 mL) was added to a suspension of as received silica (SiO_2, 10 g) in toluene (250 mL), and refluxed at 120 ℃ for 24 hours with magnetic stirring. Functionalised nanoparticles were centrifuged and washed with toluene and ethanol for purification, before being dried in the oven at 80 ℃ overnight.

2.2 General SPNC formulation

Polymer was dissolved in 30 mL of a compatible solvent. Nanoparticles were added to this solution and the suspension was magnetically stirred for a minimum of 30 minutes, followed by 2 minutes of sonication to ensure complete mixing. Sonication was avoided for formulations that required heating, in order to maintain a constant temperature range. For dry formulations, the solvent was solvents were removed and captured for re-use, leaving behind a dried powder which was finely ground using a pestle and mortar before use. See table S1 below, for formulation summary.

2.3 Coating deposition

2.3.1 Spray coating

Spray-coating processes were carried out using a compression pump and airbrush gun (made by Voilamart), at a pressure of 2 bar. All spraying was carried out approximately 4 cm away from the surface. The suspension was spray coated onto glass substrates (3 layers) and coated slides were left for until fully dried.

2.3.2 Dip coating

Settings were programmed as follows: emersion rate of 1530 mm/min; emersion time of 10 seconds; withdrawing rate of 760 mm/min; drying time of 10 seconds; and 7 cycles (iterations). A glass substrate was suspended from a height of 30 cm and mechanically moved into the suspension which resided directly below. After all iterations were complete, the coated substrates were left to air dry for 10 minutes.

2.3.3 Hot press

The instrument (a parallel plate hot press) was pre-set to 180 ℃. A layer of composite powder was manually deposited onto the substrate, which was then inserted between the plates of the hot press (bottom plate unheated; coating facing towards heated plate). The press was closed for a period of 30 seconds. This was repeated a total of three times with an additional layer of powder being applied each time, and any excess coating being removed between each iteration by streaming nitrogen gas over the surface.

UV degradation Process: Samples were exposed to UV irradiation using a UV lamp of 365nm wavelength, which was situated 6.8 cm above coated slides.

S2 Movies

Movie S1. Water bouncing TiO_2-PDMS ($\mathbf{r}_{sphere}$ = 10.5 nm, $\mathbf{r}_{poly}$ = 6 nm)

A high speed camera (1000 frames per second) was used to film in the interaction of water. 6 μL water droplets were dispensed directly from a 27 gauge dispensing tip positioned 20 mm above the substrate surface. 12+ bounces were observed.

Movie S2. Finger wipe SiO_2-PDMS ($\mathbf{r}_{sphere}$ = 7.5 nm, $\mathbf{r}_{poly}$ = 5 nm)

Movie S3. Finger wipe SiO_2-FAS ($\mathbf{r}_{sphere}$ = 7.5 nm)

Movie S4. Self-cleaning test SiO_2-PDMS ($\mathbf{r}_{sphere}$ = 7.5 nm, $\mathbf{r}_{poly}$ = 2 nm)

Movie S5. Self-cleaning test SiO_2-PDMS ($\mathbf{r}_{sphere}$ = 7.5 nm, $\mathbf{r}_{poly}$ = 10 nm)

Water was dyed with methylene blue to aid visualisation in all videos. Manganese dioxide (MnO_2) was used to simulate dirt.

S3 SPNC overview & WCA data

Table S1. SPNC formulation summary detailing the fundamental details of each individual formulation and showing the $\mathbf{r}_{poly}$ range and optimal $\mathbf{r}_{poly}$ for formulation systems that were explored in detail. The SPNC design principle (reported in the manuscript) was used to calculate weights from theoretical polymer thicknesses, see example below.

Nanoparticle	$\mathbf{r}_{sphere}$ (nm)	Polymer	Solvent system	Pre-functionalisation	Deposition Technique	Model system r_{poly} range (nm)	Optimal $\mathbf{r}_{poly}$ (nm)
TiO_2	10.5	PDMS	Hexane/Ethanol	-	Spray coat	2-8	4
SiO_2	7.5	PDMS	Hexane	HMDS	Spray coat	2-10	5
SiO_2	125	PDMS	Hexane	HMDS	Spray coat	30-120	80
SiO_2	7.5	Polyethylene	Xylene	HMDS	Dip Coat	1.5-5	1.5
SiO_2	7.5	PVC	Tetrahydrofuran	HMDS	Hot press	-	1.5
SiO_2	7.5	PVC	Tetrahydrofuran	HMDS	Spray coat	-	1.5
SiO_2	7.5	Polypropylene	Xylene	HMDS	Dip coat	-	1.5
CeO_2	12.5	PDMS	Hexane/Ethanol	-	Spray coat	-	7.5

Nanoparticle mass (g)	Polymer mass (g)	Solvent volume	Deposition temperature range (°C)	WCA Table #	SEM Figure #
0.23	Varied with r_{poly}	10 mL ethanol/ 10 mL hexane	-	S2	S9/S10
0.2	Varied with r_{poly}	30 mL hexane	-	S3	S11
0.4	Varied with r_{poly}	60 mL hexane	-	S4	S12
Varied with r_{poly}	0.1	70 mL xylene	83-87	S5	S13
Varied with r_{poly}	0.1	30 mL THF	-	-	S14
Varied with r_{poly}	0.1	30 mL THF	-	S6	S15
Varied with r_{poly}	0.1	70 mL xylene	68-70	S7	S16
0.5	Varied with r_{poly}	10 mL ethanol/ 10 mL hexane	-	S8	S17

**Formulations comprising thermoset polymers (PDMS sylgard-184, 10:1 mass ratio of base and curing agent) use a constant starting mass of nanoparticles, and formulations comprising thermoplastics (polyethylene, PVC, polypropylene) use a constant starting mass of polymer. The SPNC design principle was used to calculate the mass of the other component for each desired polymer thickness.*

Example SPNC design principle (15 nm nanoparticle with an r_{poly} of 4 nm) – converting a theoretical polymer thickness to a mass ratio.

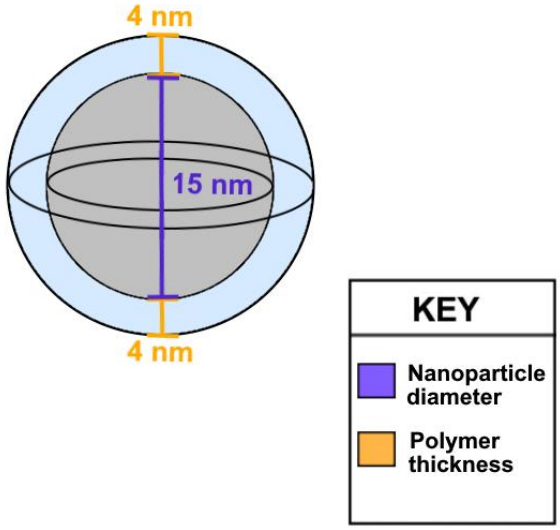

$Volume_{(sphere + poly)} = 4/3\pi*(r_{sphere + poly} * 10^{-9})^3$ *e.g.* $r_{sphere + poly} = 11.5$

$Volume_{(sphere)} = 4/3\pi*(r_{sphere} * 10^{-9})^3$ *e.g.* $r_{sphere} = 7.5$

$Volume_{(poly)} = Volume_{(sphere + poly)} - Volume_{(sphere)}$

$Mass_{(sphere)} = Volume_{(sphere)} * Density_{(sphere)}$

$Mass_{(poly)} = Volume_{(poly)} * Density_{(poly)}$

$Mass\ ratio = Mass_{(poly)} / Mass_{(sphere)}$

Model systems:

Table S2. $\mathbf{r}_{poly}$ vs WCA for TiO_2-PDMS ($\mathbf{r}_{sphere}$ = 10.5 nm).

$\mathbf{r}_{poly}$ (nm)	WCA
2	164.9° ± 2
4	165.5° ± 2
6	164.5° ± 1
7	164.3° ± 1
8	162.6° ± 2

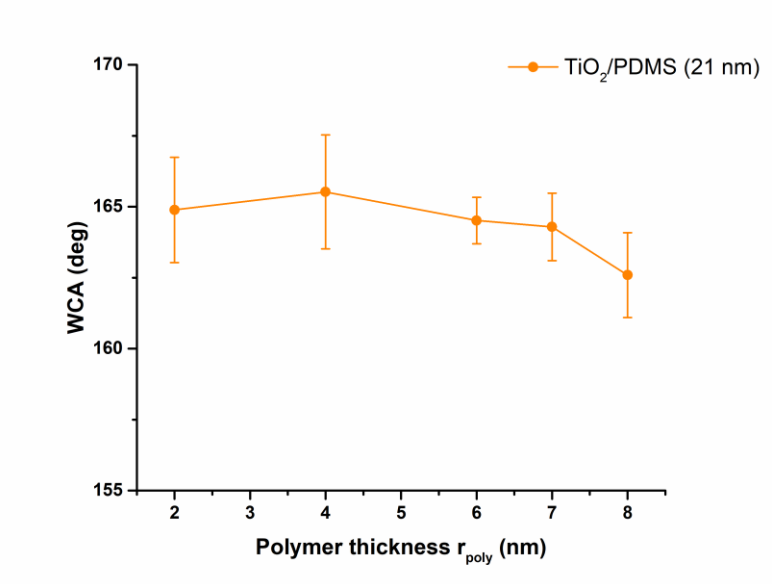

Table S3. $\mathbf{r}_{poly}$ vs WCA for SiO_2-PDMS ($\mathbf{r}_{sphere}$ = 7.5 nm).

$\mathbf{r}_{poly}$ (nm)	WCA
2	161.0° ± 1
4	163.7° ± 2
5	167.3° ± 2
6	165.1° ± 1
7	135.1° ± 12
8	134.7° ± 11
10	112.1° ± 13

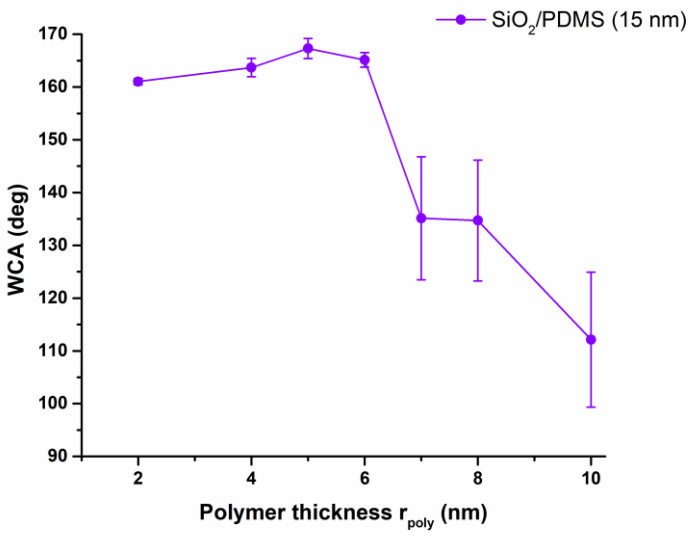

Table S4. $\mathbf{r}_{poly}$ vs WCA for SiO_2-PDMS ($\mathbf{r}_{sphere}$ = 125 nm).

$\mathbf{r}_{poly}$ (nm)	WCA
30	160.2° ± 2
50	160.2° ± 4
70	160.8° ± 2
80	161.3° ± 3
100	121.5° ± 7
120	119.5° ± 12

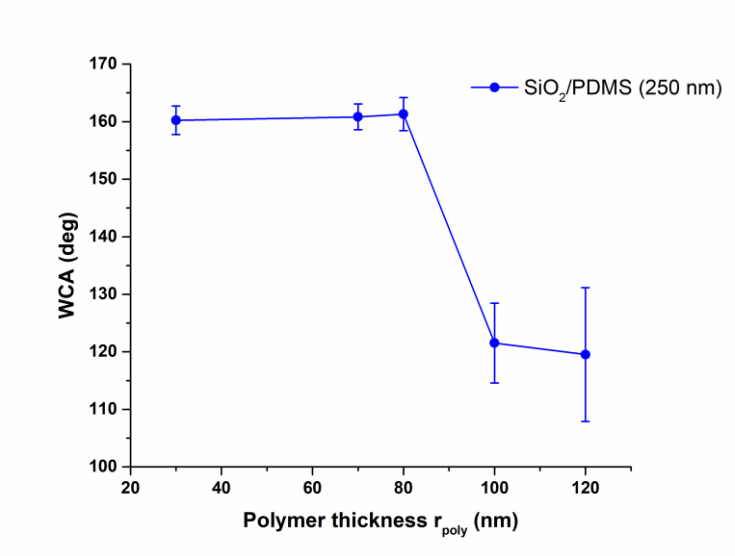

Table S5. $\mathbf{r}_{poly}$ vs WCA for SiO_2-polyethylene ($\mathbf{r}_{sphere}$ = 7.5 nm).

$\mathbf{r}_{poly}$ (nm)	WCA
1.5	164.9° ± 2
2	161.7° ± 3
3	160.6° ± 2
4	153.7° ± 7
5	143.4° ± 6

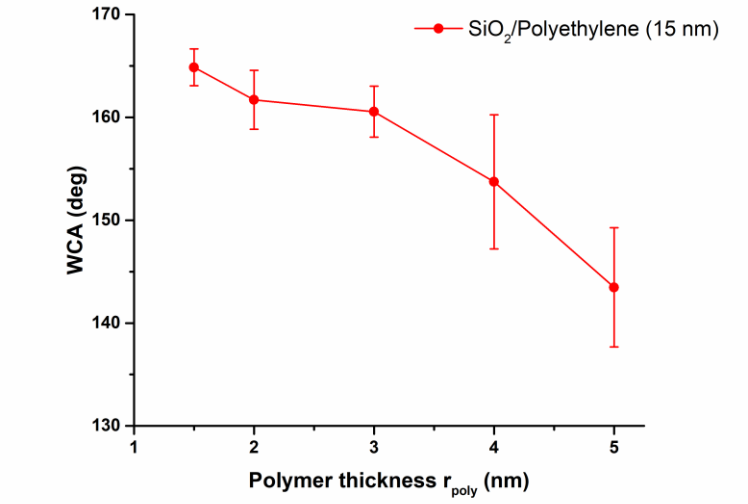

Other example systems:

Table S6. $\mathbf{r}_{poly}$ vs WCA for SiO_2-PVC ($\mathbf{r}_{sphere}$ = 7.5 nm).

$\mathbf{r}_{poly}$ (nm)	WCA
1.5	164.8° ± 1
4	144° ± 8
6	107.2° ± 6

Table S7. $\mathbf{r}_{poly}$ vs WCA for SiO_2-polypropylene ($\mathbf{r}_{sphere}$ = 7.5 nm).

$\mathbf{r}_{poly}$ (nm)	WCA
1.5	166.8° ± 3
2	163.4° ± 2
3	163.7° ± 1

Table S8. $\mathbf{r}_{poly}$ vs WCA for CeO_2-PDMS ($\mathbf{r}_{sphere}$ = 12.5 nm).

$\mathbf{r}_{poly}$ (nm)	WCA
7.5	165.1° ± 1

S4 Physical resilience molecular vs polymeric (SiO_2-FAS vs SiO_2-PDMS)

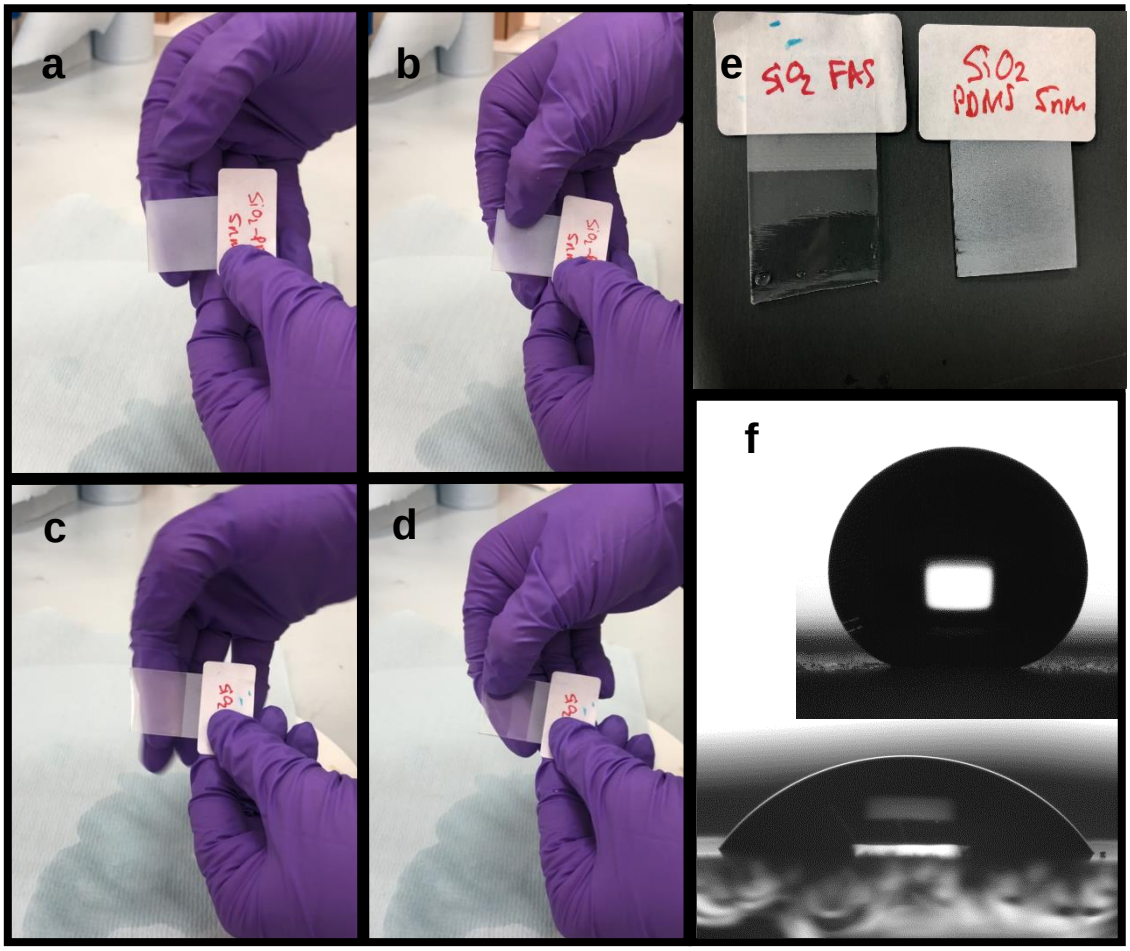

Fig. S1. (a, b) SiO_2-PDMS ($\mathbf{r}_{sphere}$ = 7.5 nm, $\mathbf{r}_{poly}$ = 5 nm) before and after finger wipe. (c, d) SiO_2-FAS ($\mathbf{r}_{sphere}$ = 7.5 nm) before and after finger wipe. (e) both samples after finger wipe. (f) water droplets on (**top**) SiO_2-PDMS and (**bottom**) SiO_2-FAS after finger wipe.

Table S9. WCA's after finger wipe.

Finger wipe	SiO_2-PDMS	SiO_2-FAS
Before	167.3° ± 2	158.9° ± 3
After	162.8° ± 1	61.4° ± 3

S5 Physical resilience hot pressed SiO_2-PVC

Samples were subject to an arbitrary robustness test to assess their mechanical durability. The weighted sample (100g), attached to a glass support, was placed coating down and pushed 10 cm across sandpaper, turned by 90° and pushed a further 10 cm to complete one cycle (standard sand paper, grit no. 120).

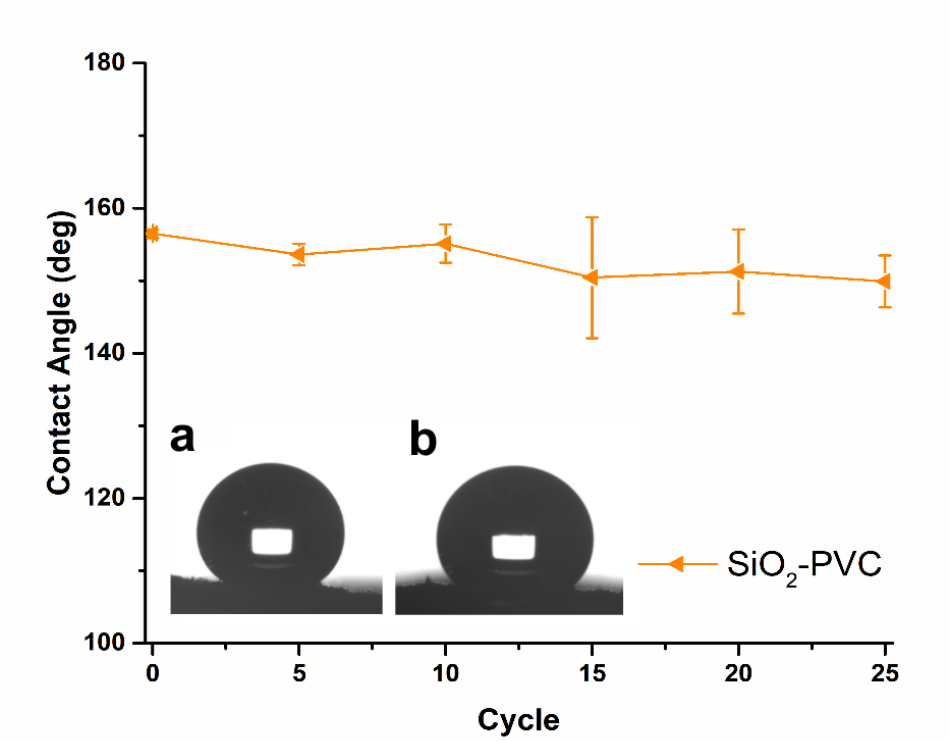

Fig. S2. A graph to show the variation in WCA of SiO_2-PVC films hot pressed into PVC-coated fabric substrates ($\mathbf{r}_{sphere}$ = 7.5, polymer thickness 1.5 nm), during 25 cycles of physical abrasion with sandpaper of grit no. 120. Inset shows images of a water droplet on these surfaces (a) before and (b) after abrasion.

Table S10. WCA's before and after abrasion cycles.

Cycles	WCA
0	156.5° ± 1
25	150° ± 4

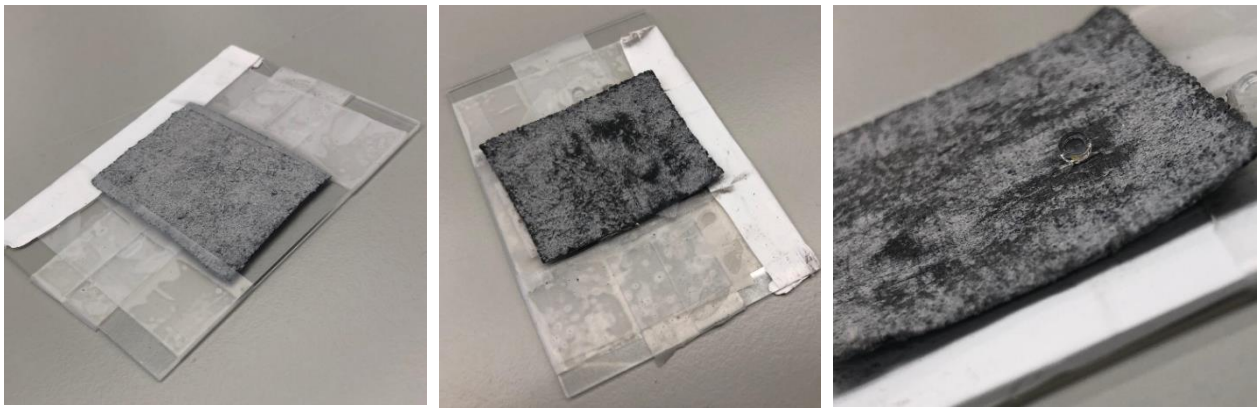

Fig. S3. Hot pressed SiO_2-PVC films before physical abrasion (left), after 25 cycles of abrasion (middle) and showing a water droplet resting on the surface after 25 cycles of abrasion (right).

S6 Focused ion beam data

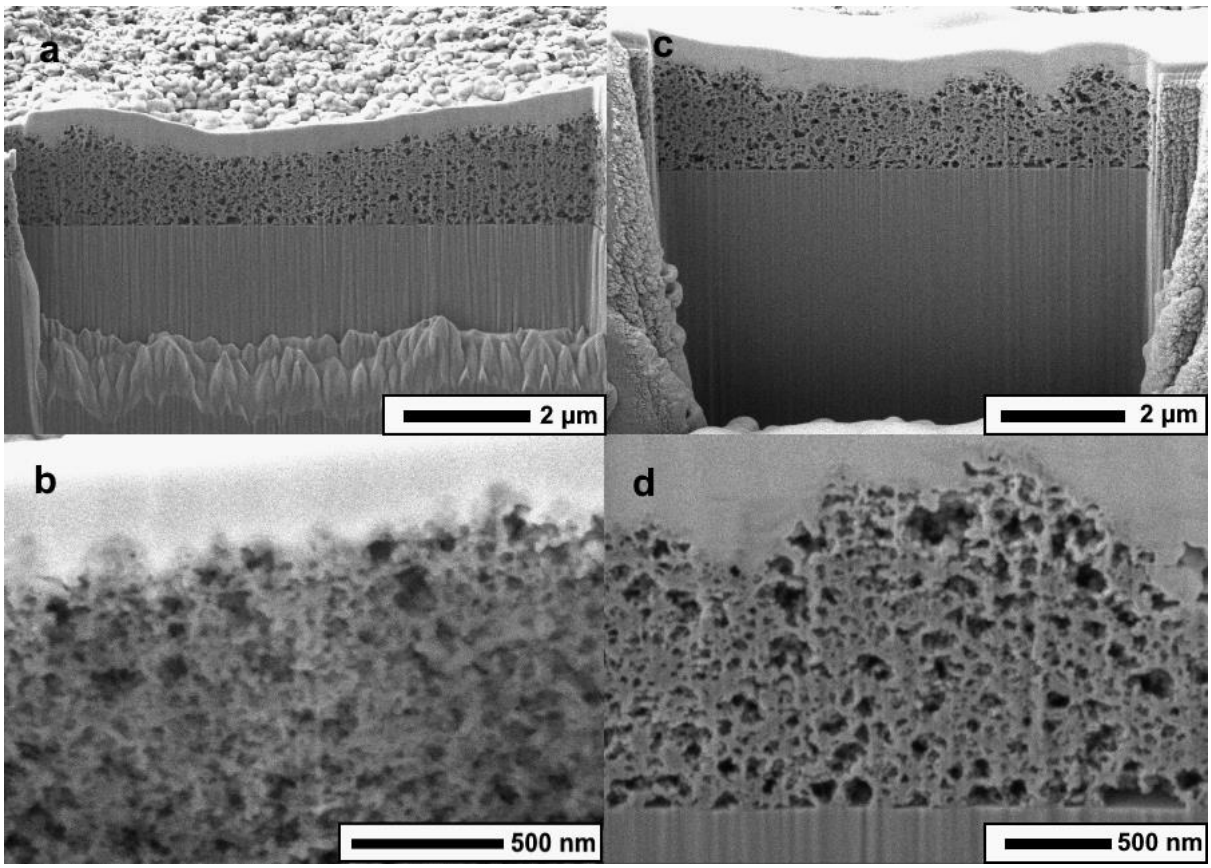

Fig. S4. Secondary electron micrographs of FIB-prepared cross-sections of SiO_2-PVC cross sections, prepared on silicon wafer *via* spray coating and platinum strap applied to the surface before milling for protection; (a, b) 15 nm nanoparticle diameter and (c, d) 250 nm nanoparticle diameter at low and high magnifications. Scale bars are shown.

S7 Confocal fluorescence microscopy

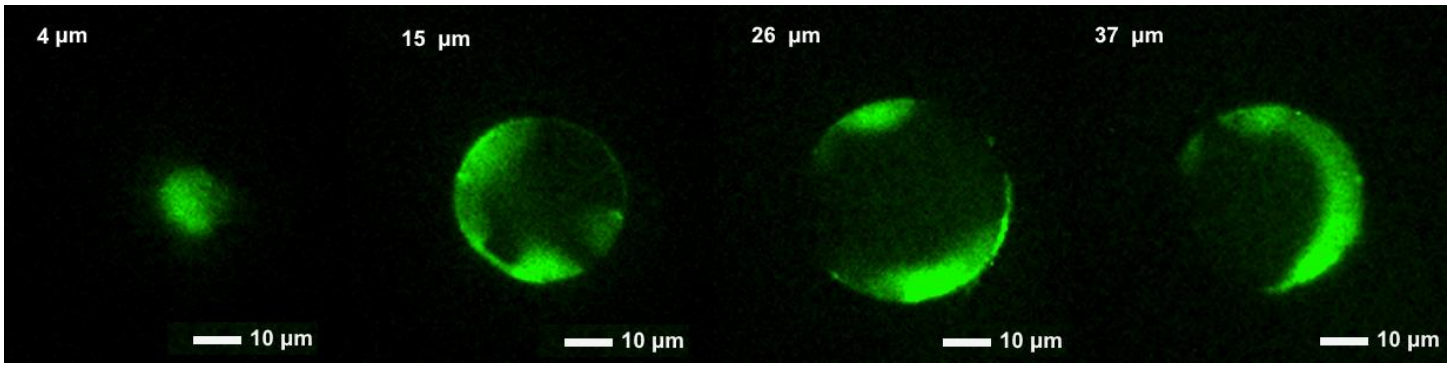

Fig. S5. Confocal fluorescent microscopy images of SiO_2-PVC SPNC (40-75 µm SiO_2 particles; PVC stained with fluorescent dye Lucigenin); z-stack images of slices at 4, 15, 26 and 37 µm.

Conformal coatings were not observed for thermoplastic systems, but instead incomplete coverage with polymer was seen, as a result of the solvent evaporation process. It is clear from the z-stack images that the dye accumulates in areas surrounding the SiO_2 particle (dark centre).

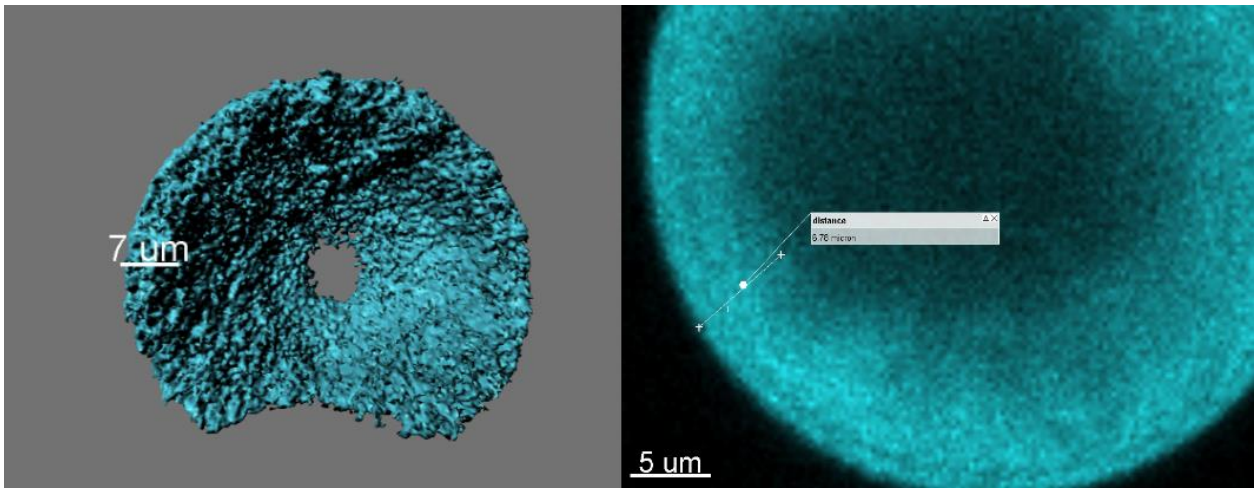

Fig. S6. Confocal fluorescent microscopy images of SiO_2-PDMS SPNC (40-75 µm SiO_2 particles; PDMS stained with fluorescent dye NR). (**left**) 3D-model of the cross-sectional shell of a single particle; (**right**) z-stack slice at 29 µm.

Fig. S6 depicts attempts of measuring the polymer shell thickness for a SiO_2-PDMS composite particle, from the raw data (**right**) and as a 3D-model (**left**), obtained by segmentation and surface rendering of the raw data. Thicknesses tend to vary between different points in the same representation, and also vary between representations for reasons discussed in the manuscript. For a ~40 µm diameter particle, a polymer shell thickness of ~ 10-11 µm was anticipated

(scaling up from a 15 nm SiO_2 nanoparticle: 4 nm PDMS shell). However, most measurements were in the region of 6-8 μm, which was slightly thinner than expected.

S8 UV degradation tests

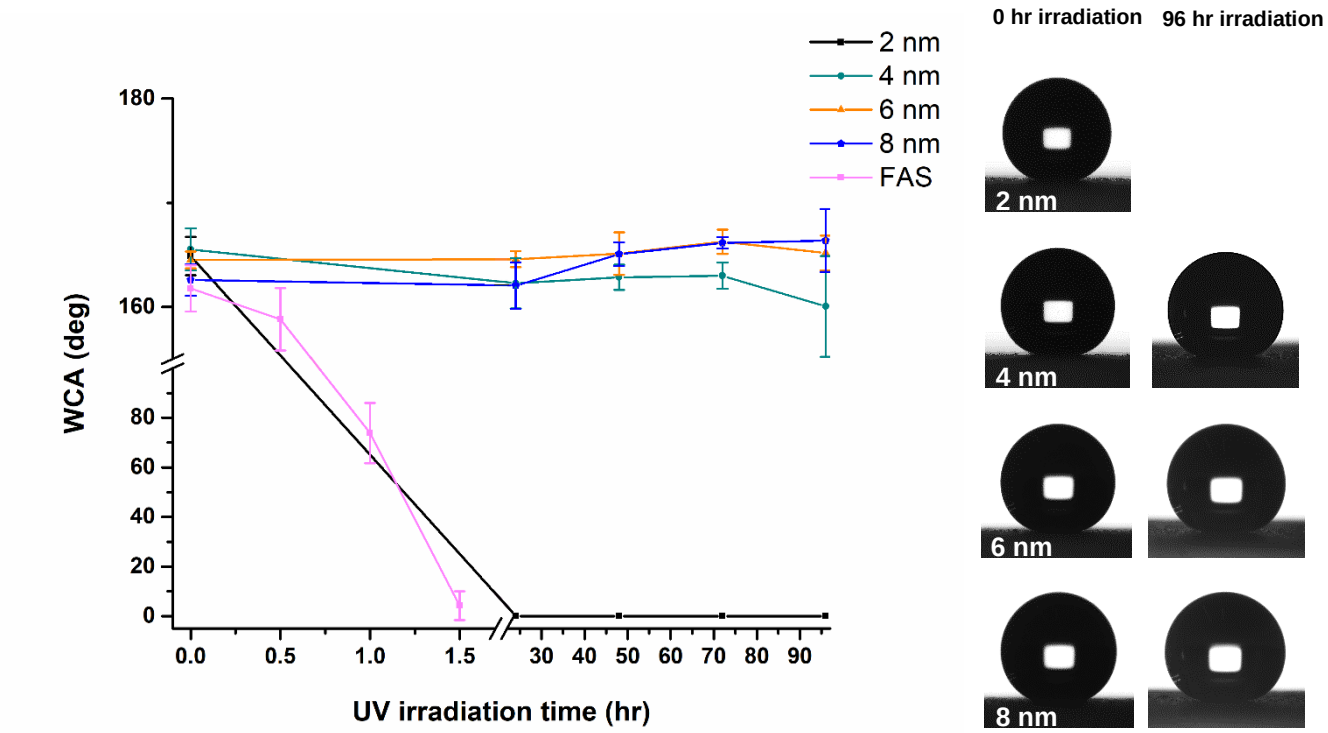

Fig. S7. (**left**) a graph to show how the WCA of TiO_2-PDMS (polymer thickness of 2 nm, 4 nm, 6 nm and 8 nm) and TiO_2-FAS changes over time when irradiated (365 nm). (**right**) water droplets on TiO_2-PDMS surfaces at 0 hours and after 96 hours of irradiation.

Table S11. WCA's of SiO_2-PDMS after 96 hours of irradiation.

SiO_2-PDMS $\mathbf{r}_{poly}$ (nm)	WCA after 96 hr irradiation
2	0
4	160.1° ± 5
6	165.2° ± 2
8	166.4° ± 3

S9 Self-cleaning tests

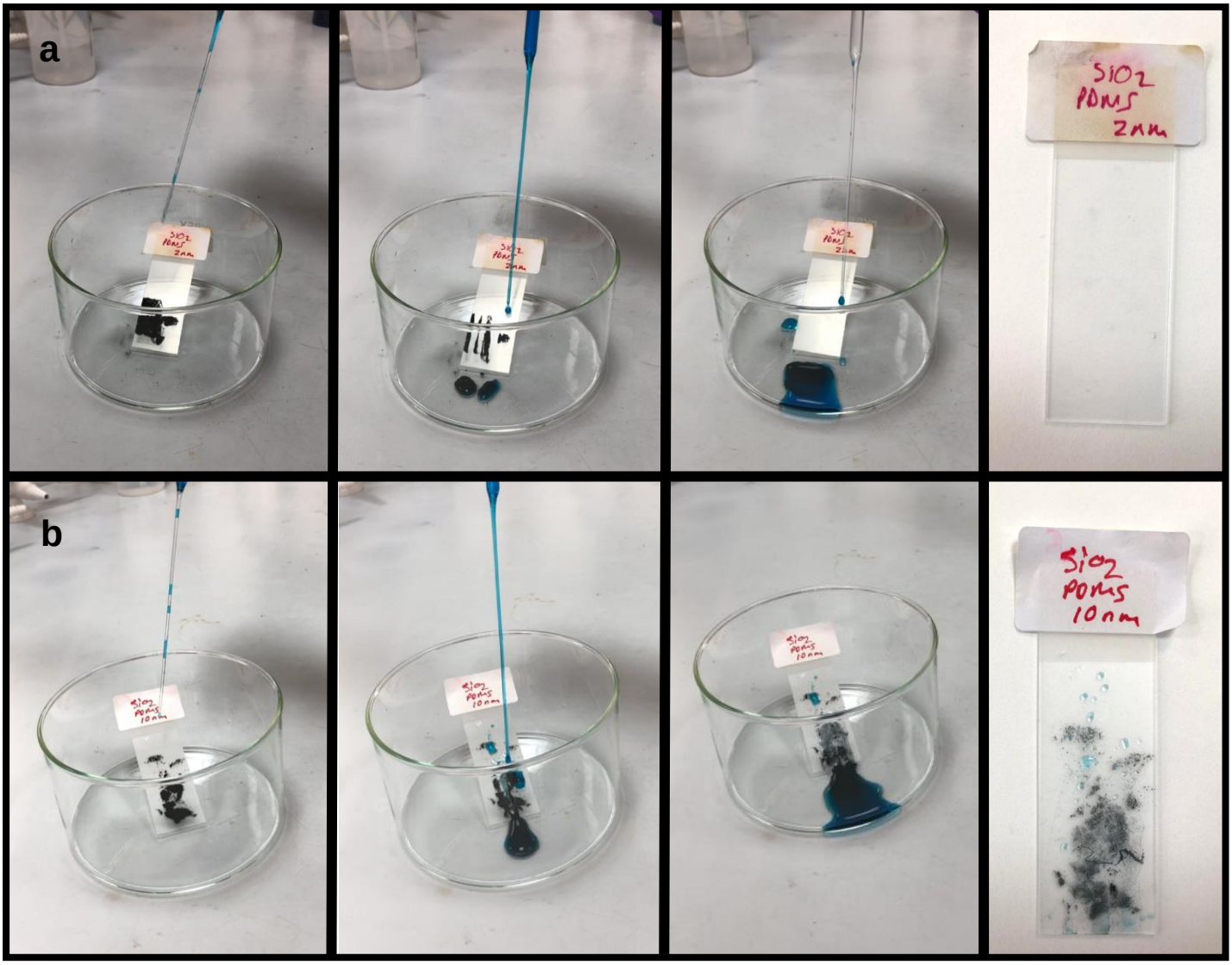

Fig. S8. Self-cleaning tests before, during and after the removal of 'dirt' (MnO_4) from the coating surface by water (dyed with methylene blue to aid visulisation, Lotus effect); (a) SiO_2-PDMS ($\mathbf{r}_{sphere}$ = 7.5 nm**,** $\mathbf{r}_{poly}$ = 2 nm) and (b) SiO_2-PDMS ($\mathbf{r}_{sphere}$ = 7.5 nm**,** $\mathbf{r}_{poly}$ = 10 nm).

S10 SPNC SEM

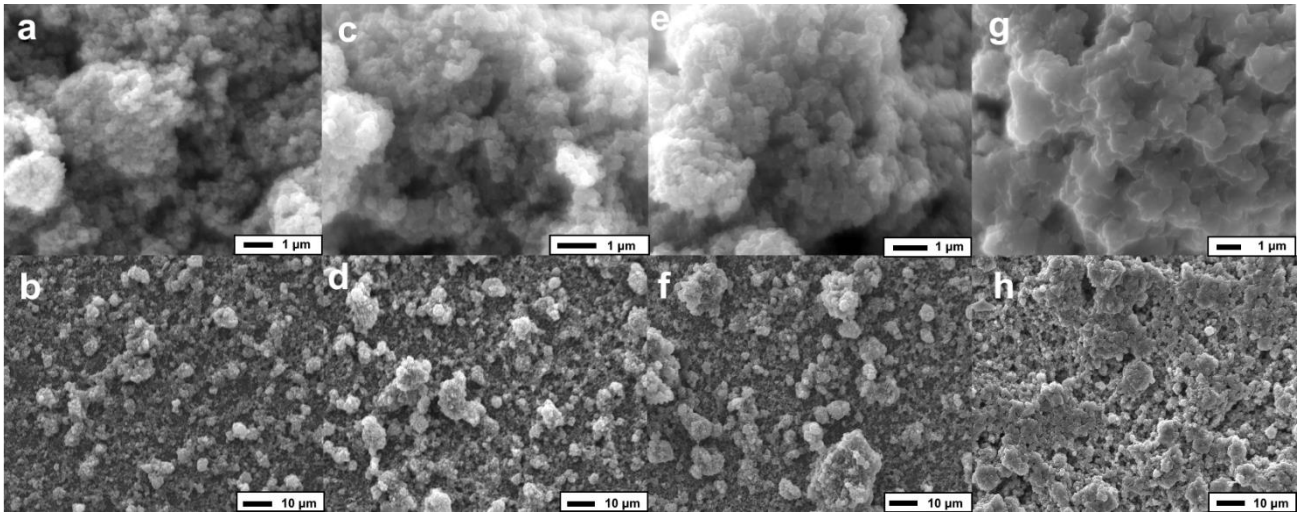

Fig. S9. Micrographs of TiO_2-PDMS surface morphology ($\mathbf{r}_{sphere} = 10.5$ nm); polymer thickness of (a, b) 4 nm, (c, d) 6 nm, (e, f) 8 nm and (g, h) 10 nm at low and high magnification. Scale bars are shown.

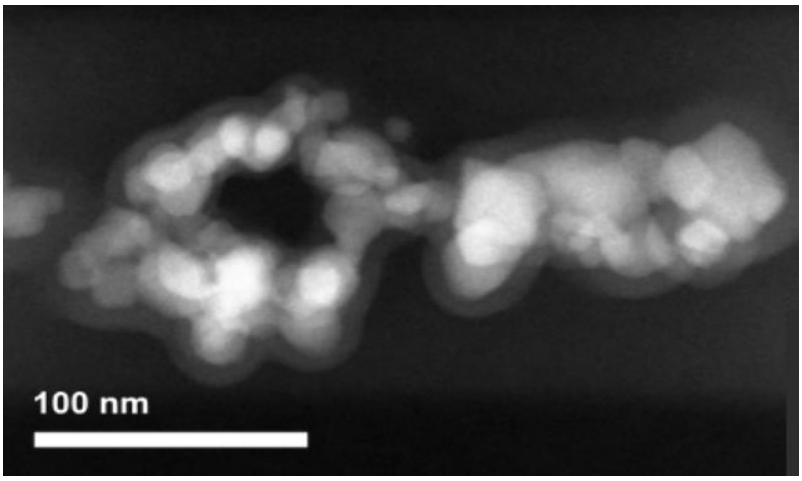

Fig. S10. Scanning-transmission electron microscopy (S-TEM) image of TiO_2-PDMS ($\mathbf{r}_{sphere} = 10.5$ nm), with polymer thickness of 7 ± 2 nm. Scale bar are shown.

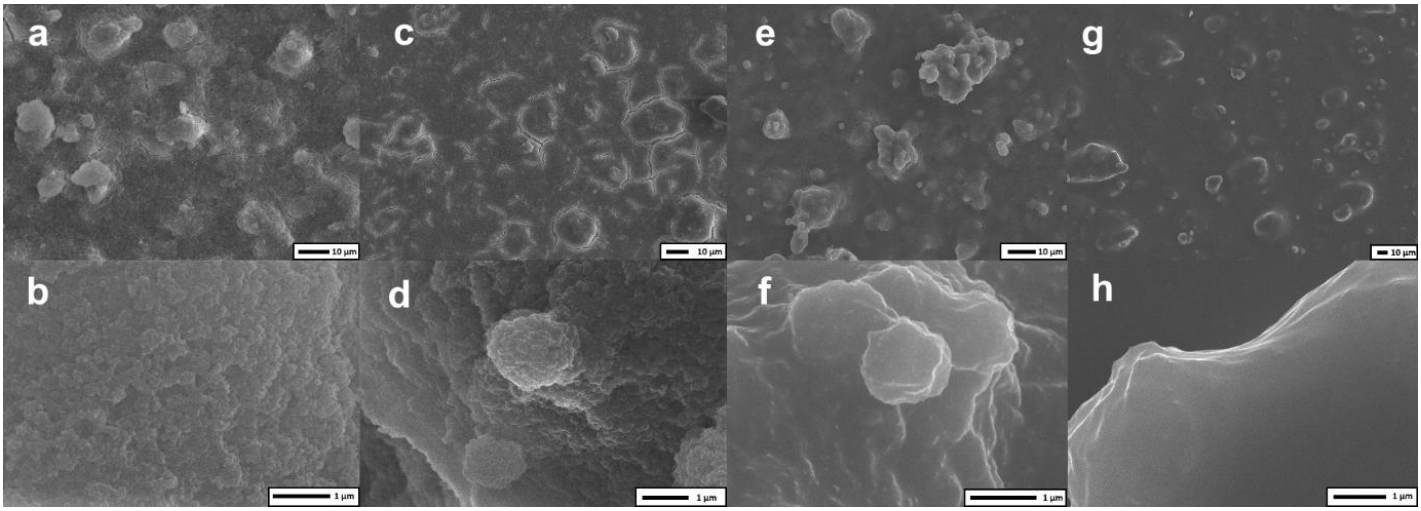

Fig. S11. Micrographs of SiO_2-PDMS surface morphology ($\mathbf{r}_{sphere}$ = 7.5 nm); polymer thickness of (a, b) 4 nm, (c, d) 6 nm, (e, f) 8 nm and (g, h) 10 nm at low and high magnification. Scale bars are shown.

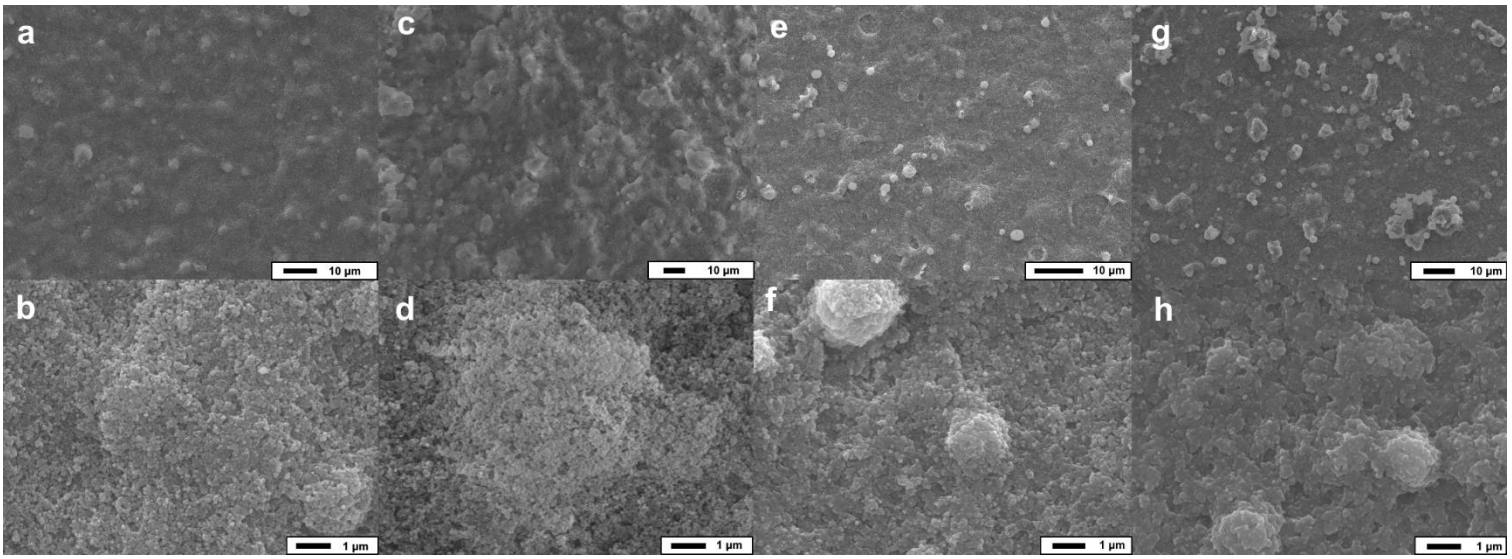

Fig. S12. Micrographs of SiO_2-PDMS surface morphology ($\mathbf{r}_{sphere}$ = 125 nm); polymer thickness of (a, b) 50 nm, (c, d) 80 nm, (e, f) 100 nm and (g, h) 120 nm at low and high magnification. Scale bars are shown.

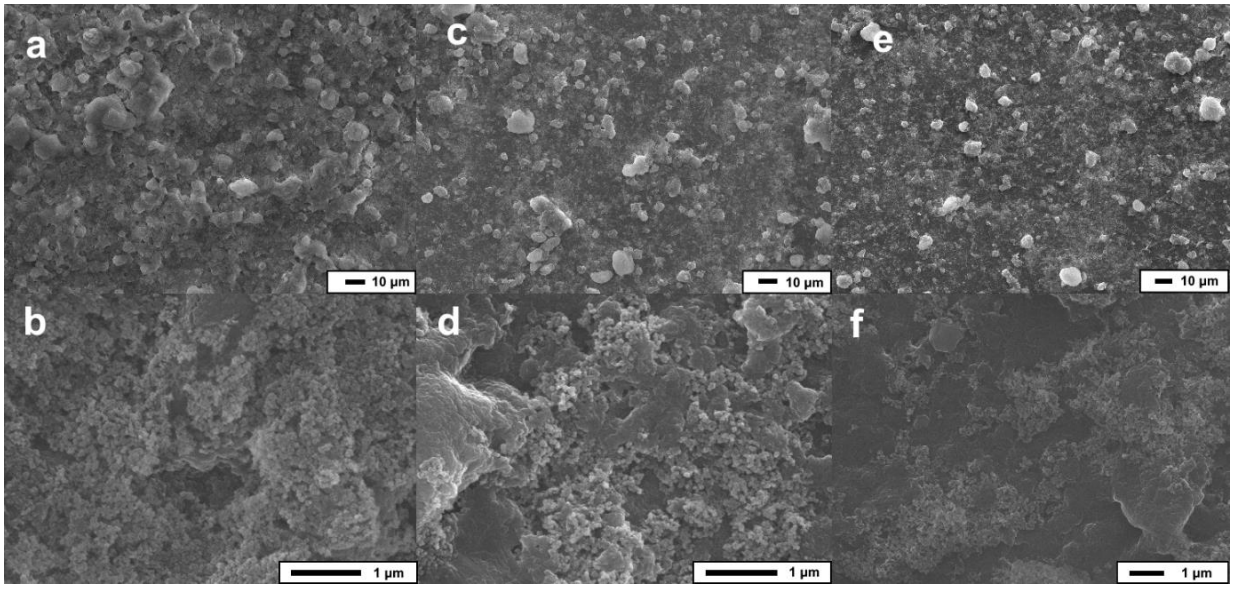

Fig. S13. Micrographs of SiO_2-polyethylene surface morphology ($\mathbf{r}_{sphere} = 7.5$ nm); polymer thickness of (a, b) 1.5 nm, (c, d) 2 nm and (e, f) 3 nm at low and high magnification. Scale bars are shown.

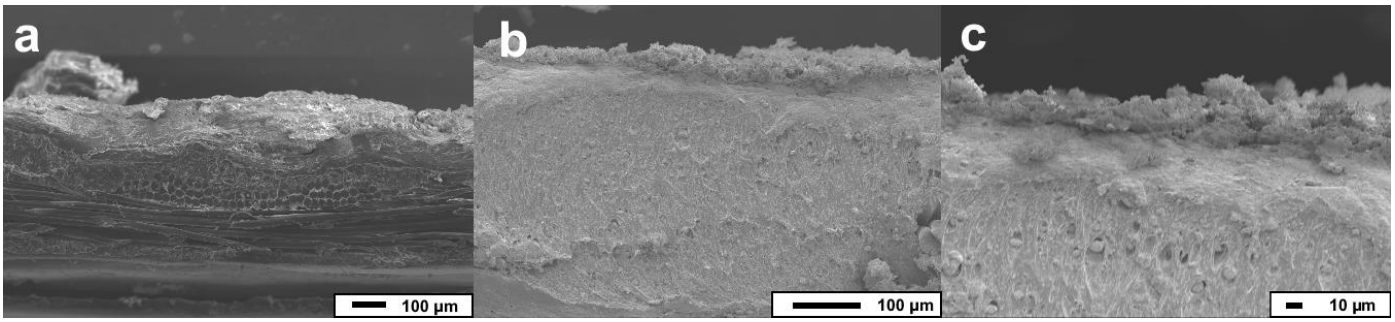

Fig. S14. Cross sectional micrographs of SiO_2-PVC ($\mathbf{r}_{sphere} = 7.5$ nm) hot pressed into PVC-coated fabric substrate, prepared by cutting; polymer thickness of 1.5 nm, at different magnifications. Scale bars are shown.

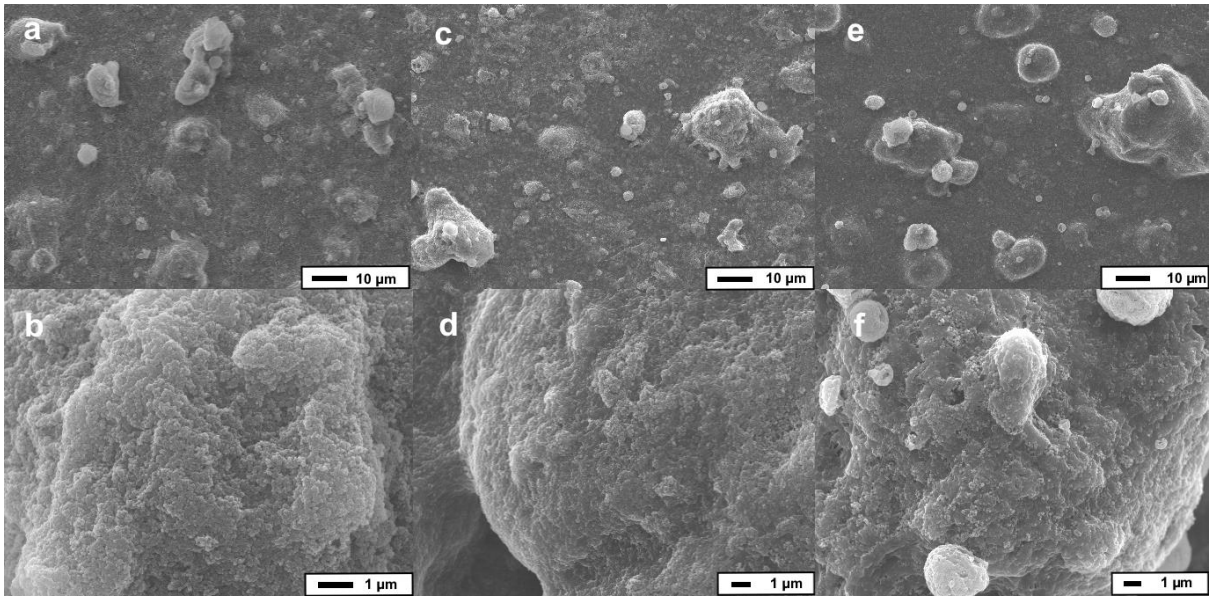

Fig. S15. Micrographs of SiO_2-PVC surface morphology ($\mathbf{r}_{sphere}$ = 7.5 nm); polymer thickness of (a, b) 1.5 nm, (c, d) 4 nm and (e, f) 6 nm at low and high magnification. Scale bars are shown.

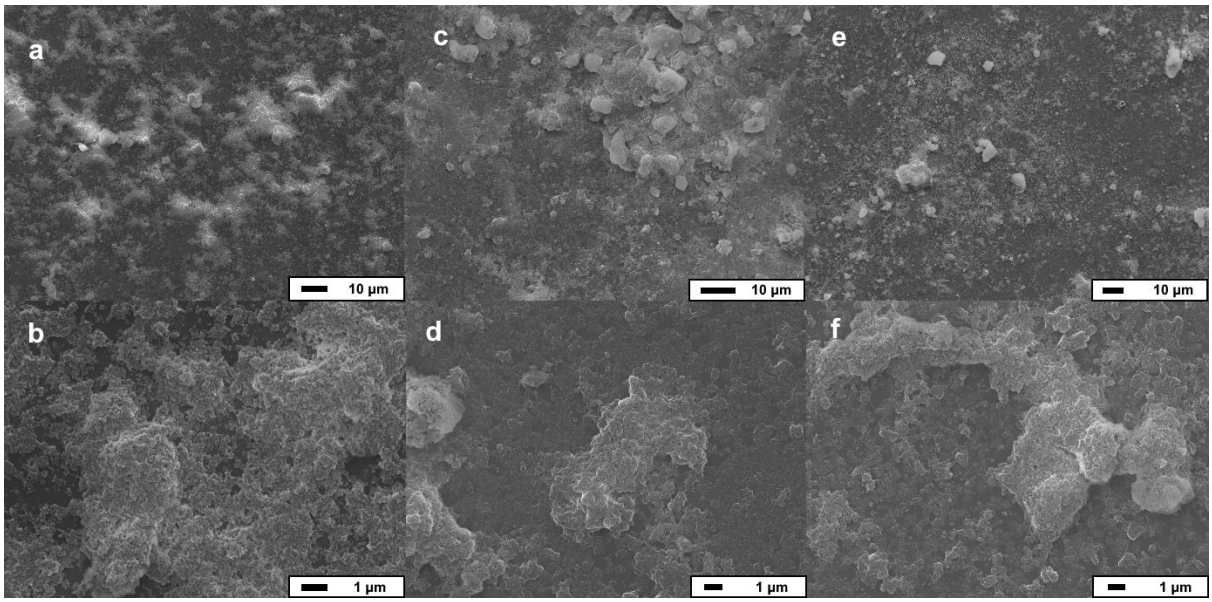

Fig. S16. Micrographs of SiO_2-polypropylene surface morphology ($\mathbf{r}_{sphere}$ = 7.5 nm); polymer thickness of (a, b) 1.5 nm, (c, d) 2 nm and (e, f) 3 nm at low and high magnification. Scale bars are shown.

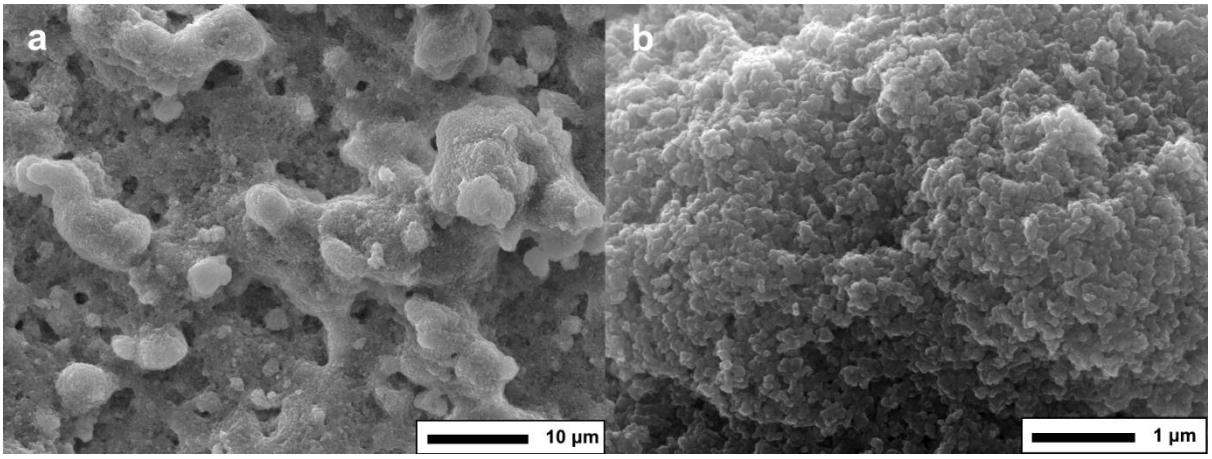

Fig. S17. Micrographs of CeO_2-PDMS surface morphology ($\mathbf{r}_{sphere}$ = 12.5 nm); polymer thickness of 7.5 nm, at low and high magnification. Scale bars are shown.

S11 SPNC FTIR

Functionalisation of SiO_2 with HMDS: FTIR was used to confirm the functionalisation of SiO_2 nanoparticles with HMDS. Unfunctionalised silica displayed a signal at 3650 cm^{-1}, representative of surface –OH groups, and at 1100 cm^{-1} which is characteristic of Si-O-Si, stretching, respectively.[3] Post functionalisation, a reduction in intensity of the band representative of –OH can be observed. This is owed to the displacement of surface hydroxyl groups by trimethylsilyl groups. Furthermore, a band observed at ~2980 cm^{-1} can be assigned to the stretching frequency of –CH3 groups, in addition to bands at ~870 cm^{-1} and ~750 cm^{-1} corresponding to Si-C stretching.[4]

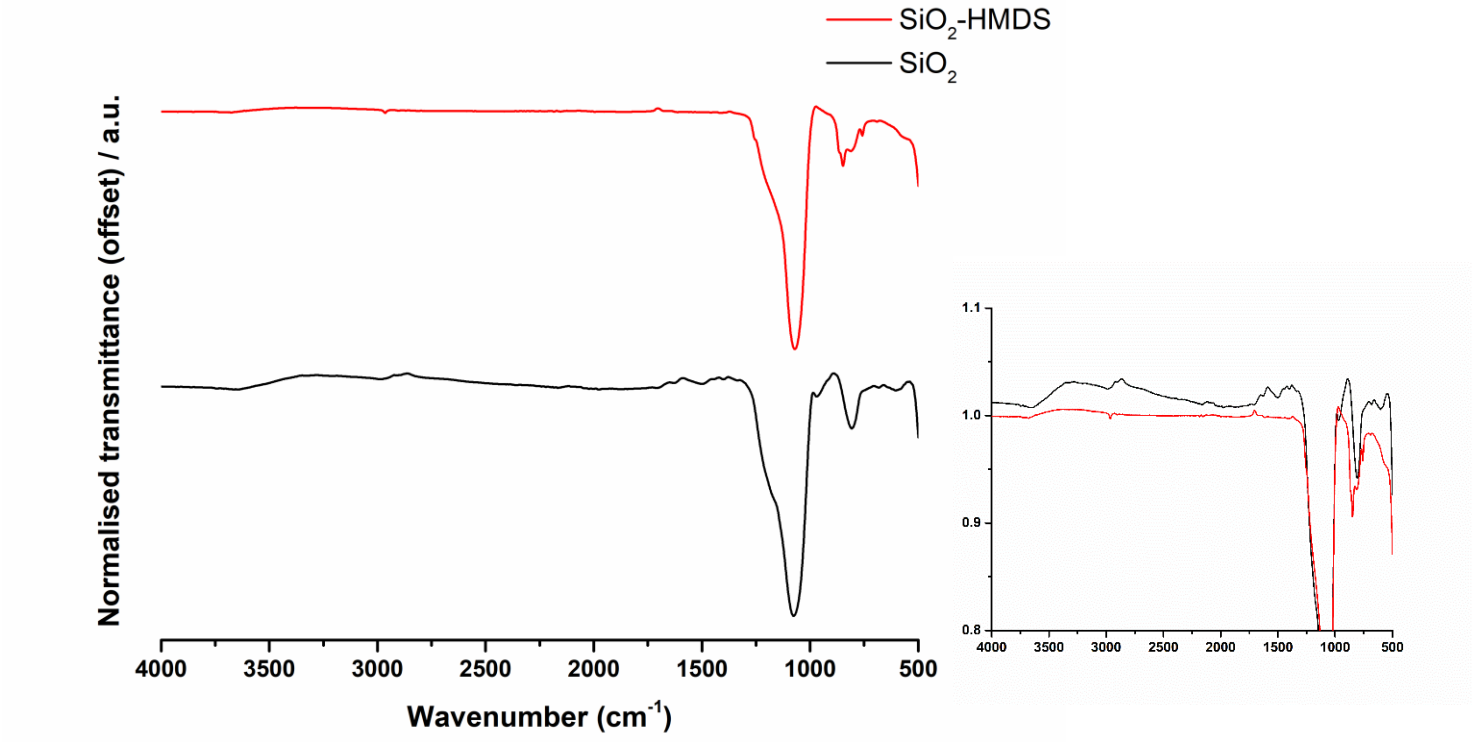

Fig. S18. FTIR of unfunctionalised SiO_2 ($\mathbf{r}_{sphere}$ = 7.5 nm, black) and HMDS-functionalised SiO_2 ($\mathbf{r}_{sphere}$ = 7.5 nm, red). Inset is the magnified overlaid spectra, for clarity.

Other FTIR:

PDMS: 2962 cm^{-1} representative of asymmetric CH_3 stretching in Si-CH_3, 1257 cm^{-1} characteristic of the CH_3 symmetric deformation of Si-CH_3, 1057 cm^{-1} arising from Si-O-Si stretching and 797 cm^{-1} due to the Si-C stretching vibration, respectively.[1,2] Additionally, a reduction in intensity of the band representative of –OH can be observed can be observed (3400-3200 cm^{-1}) in some spectra, owed to the functionalisation of particles with PDMS.

Polyethylene: Absorption peaks at 2916 cm^{-1} and 2848 cm^{-1}, representative of C–H asymmetric and C–H symmetric stretching vibrations, could be seen. In addition to absorption peaks at 1471 cm^{-1} and 717 cm^{-1}, owing to the C–H deformation vibrations C–C rocking vibrations in CH_2 groups.[5]

PVC: characteristic vibrational stretches can be seen at 2800-3000 cm^{-1}, representative of aliphatic C-H stretches, 2910 cm^{-1} which is distinguishing of an asymmetric methylene group C-H stretch, stretches between 1425-1200 cm^{-1} which can be assigned to C-H (H-C-Cl), 1329 cm^{-1} which is typical of the in-plane CH deformation and 958 cm^{-1} which corresponds to C-H rocking vibrations, respectively.[6] Any additional peaks correspond to the phthalate ester plasticizer within the material (where applicable).

Polypropylene: four bands present in the region 3000-2800 cm^{-1} correspond to asymmetric and symmetric alkyl C-H stretches, sharp signals at 1456 cm^{-1} and 1375 cm^{-1} can be attributed to asymmetric (1456 cm^{-1}) and symmetric (1375 cm^{-1}) CH_3- deformation vibrations, and additional signals at lower wavenumbers (1200-750 cm^{-1}) are representative of CH_3-/CH_2-rocking vibrations and C-C asymmetric and symmetric stretching vibrations. [7]

References

1 X. Zhang, H. Ye, B. Xiao, L. Yan, H. Lv and B. Jiang, *J. Phys. Chem. C*, 2010, **114**, 19979–19983.

2 L. Johnson, L. Gao, C. Shields IV, M. Smith, K. Efimenko, K. Cushing, J. Genzer and G. P López, *J. Nanobiotechnology*, 2013, **11**, 22.

3 P. G. Pai, S. S. Chao, Y. Takagi and G. Lucovsky, *J. Vac. Sci. Technol. A Vacuum, Surfaces, Film.*, 1986, **4**, 689–694.

4 S. Haukka and A. Root, *J. Phys. Chem.*, 1994, **98**, 1695–1703.

5 N. De Geyter, R. Morent and C. Leys, *Surf. Interface Anal. An Int. J. devoted to Dev. Appl. Tech. Anal. surfaces, interfaces thin Film.*, 2008, **40**, 608–611.

6 C.-Y. Loo, P. M. Young, W.-H. Lee, R. Cavaliere, C. B. Whitchurch and R. Rohanizadeh, *Acta Biomater.*, 2012, **8**, 1881–1890.

7 R. Morent, N. De Geyter, C. Leys, L. Gengembre and E. Payen, *Surf. Interface Anal. An Int. J. devoted to Dev. Appl. Tech. Anal. surfaces, interfaces thin Film.*, 2008, **40**, 597–600.